Vortex creation during magnetic trap manipulations of spinor Bose-Einstein condensates

A. P. Itin,[1,2] T. Morishita,[1] M. Satoh,[1] O. I. Tolstikhin,[3] and S. Watanabe[1]
[1]*Department of Applied Physics and Chemistry, University of Electro-Communications, 1-5-1, Chofu-ga-oka, Chofu-shi, Tokyo 182-8585, Japan*
[2]*Space Research Institute, RAS, Moscow, Russia*
[3]*Russian Research Center "Kurchatov Institute," Kurchatov Square 1, Moscow 123182, Russia*
(Received 4 April 2006; published 13 June 2006)

We investigate several mechanisms of vortex creation during splitting of a spinor Bose-Einstein condensate (BEC) in a magnetic double-well trap controlled by a pair of current carrying wires and bias magnetic fields. Our study is motivated by a recent MIT experiment on splitting BECs with a similar trap [Y. Shin *et al.*, Phys. Rev. A **72**, 021604 (2005)], where an unexpected fork-like structure appeared in the interference fringes indicating the presence of a singly quantized vortex in one of the interfering condensates. It is well known that in a spin-1 BEC in a quadrupole trap, a doubly quantized vortex is topologically produced by a "slow" reversal of bias magnetic field B_z. Since in the experiment a doubly quantized vortex had never been seen, Shin *et al.* ruled out the topological mechanism and concentrated on the nonadiabatic mechanical mechanism for explanation of the vortex creation. We find, however, that in the magnetic trap considered both mechanisms are possible: singly quantized vortices can be formed in a spin-1 BEC topologically (for example, during the magnetic field switching-off process). We therefore provide a possible alternative explanation for the interference patterns observed in the experiment. We also present a numerical example of creation of singly quantized vortices due to "fast" splitting; i.e., by a dynamical (nonadiabatic) mechanism.

DOI: 10.1103/PhysRevA.73.063615 PACS number(s): 03.75.Dg, 03.75.Nt, 03.65.Vf

I. INTRODUCTION

Coherent manipulation of matter-waves is presently a very important experimental and theoretical field. Coherent splitting of matter waves into spatially separate atomic wave packets with a well-defined relative phase is necessary for atom interferometry and quantum information processing applications. Bose-Einstein condensates (BECs) open unprecedented perspectives in this direction. Coherent splitting of a BEC was recently realized both in an optical double-well trap [1] and in a magnetic atom chip-based double-well trap [2]. In the latter experiment, the magnetic trap was produced by a pair of current carrying wires and a bias field used to control the distance between the wells [3]. An intriguing feature of this experiment was the appearance of a fork-like structure in the absorption image of interference fringes indicating creation of a singly quantized vortex in one of the wells. Thus perturbations during condensate manipulations were violent enough to generate vortices. To identify possible mechanisms for the vortex creation is an inevitable challenge for future pursuit of BEC interferometry with such a kind of experimental configuration.

Here we study two independent scenarios that could lead to vortex creation. One of them is the phase imprinting during the switching-off process (due to different decay times of magnetic fields in different spatial directions), while the other is dynamical vortex creation during fast splitting. Although the switching-off time in the MIT experiment was only about 20 μs (a duration much shorter than the inverse of any trap frequency), it is slow as compared to the Larmor frequency in the magnetic field of order of 1 G. Therefore, in principle an adiabatic imprinting might take place. On the other hand, the authors of Ref. [2] think the (topological) phase imprinting mechanism is an unlikely explanation for the vortex creation since they have never observed an interference pattern of *a doubly quantized* vortex (which is created topologically in spin-1 condensates when the zero point of the magnetic field crosses through condensates). However, we find it is possible to topologically create *singly quantized* vortices in a spin-1 condensate in the considered configuration. The topological creation of doubly quantized vortices happens due to transfer of atoms from the initially populated Ψ_{-1} component without vorticity to the Ψ_1 component (i.e, between $m=\pm 1$ components in a z-quantized basis; see Eqs. (1) and (2) for notation and Ref. [4]). In case the atoms are transferred from Ψ_{-1} to Ψ_0 component, singly quantized vortices are formed. Such a transfer could happen during the switching-off process, and we present the relevant realistic scenarios wherein an exponential decay of magnetic fields is assumed, with different decay constants for fields in different spatial directions. With parameters close to the experiment, we obtain numerically that a large part of the atoms (about half of the condensate) can be transferred to the component Ψ_0, which has singly quantized vortices around each of the two minima of the magnetic field. In contrast, when we try to obtain doubly quantized vortices by reversing bias field B_z, it turns out to be more difficult. At such short time scales, only a small part of the population is transferred to the component Ψ_1 with doubly quantized vortices, while the rest of the population is redistributed among other components. Creation of doubly quantized vortices in such a configuration requires times of the order of hundreds of microseconds.

We also present an example of dynamical vortex creation during a fast splitting. In this case, the condensate (including the Ψ_{-1} component) acquires some winding phase during the splitting process. This leads to clear fork-like structures in all the components and thus in the total density upon expansion. Although in our calculations this requires a sufficiently shorter time of splitting than that which was actually effected

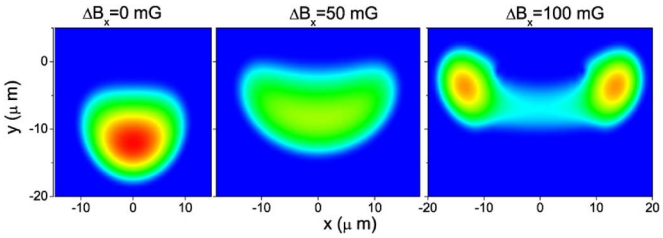

FIG. 1. (Color online) Splitting of the condensate by ramping ΔB_x from 0 to 100 mG. Total density is shown. The origin of the coordinates is the merge point without gravity. Parameters are close to the experiment of Shin *et al.*; splitting was fast: time of splitting about 5 ms.

in the real experiment [2], it might be caused by the oversimplified model (without jitter or fluctuations of the magnetic field, etc). We use a perfectly symmetric magnetic field configuration, so that vortices always appear in pairs in our calculations. Nonadiabatic dynamical mechanism leads to a vortex-antivortex pair, while the topological mechanism to a vortex-vortex pair. The real experimental setup suffered some asymmetry due to imperfections of the wires, so that the creation of a single vortex was possible.

The rest of the paper is organized as follows. In Sec. II we introduce the model [spinor BEC described by the two-dimensional (2D) GP equation with spin degrees of freedom], describe the configuration of the magnetic field produced by the two-wire setup, and its weak- and strong-field seeking states. In Sec. III, we present numerical results on vortex creation in the system. In Sec. III A we study several examples of how an unexpected topological phase imprinting could have taken place in the MIT experiment. There we take into account gravity and use realistic parameters relevant to the experiment. We assume that after switching off the magnetic field the B_z field decays faster than transversal magnetic field $B_\perp$, which can lead to the phase imprinting. In Sec. III B we present examples of dynamical vortex creation during the splitting process. When split slowly in 30 ms, the condensate develops no vortex. However, reducing the splitting duration to about 5 ms leads to vortices. Then, even in the case wherein the switching-off process leaves all population in the initial Ψ_{-1} component, expansion of condensates produces very clear forks in the interference pattern.

II. THE MODEL

A. Spinor Bose condensate

We consider a BEC of alkali atoms with hyperfine spin $F=1$ using the z-quantized basis [5]. The order parameter is expanded as

$$\Psi = \sum_{m=\pm 1,0} \Psi_m |m\rangle, \tag{1}$$

where $|m\rangle$ are eigenvectors of F_z:

$$|1\rangle = (1,0,0)^T, \quad |0\rangle = (0,1,0)^T, \quad |-1\rangle = (0,0,1)^T. \tag{2}$$

We use the time-dependent form of the GP equation with spin degrees of freedom developed in Ref. [4]:

$$i\frac{\partial}{\partial t}\Psi_j = \left[-\frac{\hbar^2}{2M}\nabla^2 + g_n \sum_l |\Psi_l|^2 + V(\mathbf{r})\right]\Psi_j + \left\{g_s \sum_\alpha \sum_{lpk} [\Psi_l^*(F_\alpha)_{lp}\Psi_p](F_\alpha)_{jk} - \mathcal{B}_{jk}\right\}\Psi_k,$$

$$\mathcal{B}_{jk} = \begin{pmatrix} B_z & \frac{B_x - B_y}{\sqrt{2}} & 0 \\ \frac{B_x + B_y}{\sqrt{2}} & 0 & \frac{B_x - B_y}{\sqrt{2}} \\ 0 & \frac{B_x + B_y}{\sqrt{2}} & -B_z, \end{pmatrix}, \tag{3}$$

where $F_\alpha(\alpha = x, y, z)$ are the angular momentum operators in the basis of the eigenvectors of F_z:

$$F_x = \frac{1}{\sqrt{2}}\begin{pmatrix} 0 & 1 & 0 \\ 1 & 0 & 1 \\ 0 & 1 & 0 \end{pmatrix}, \quad F_y = \frac{i}{\sqrt{2}}\begin{pmatrix} 0 & -1 & 0 \\ 1 & 0 & -1 \\ 0 & 1 & 0 \end{pmatrix},$$

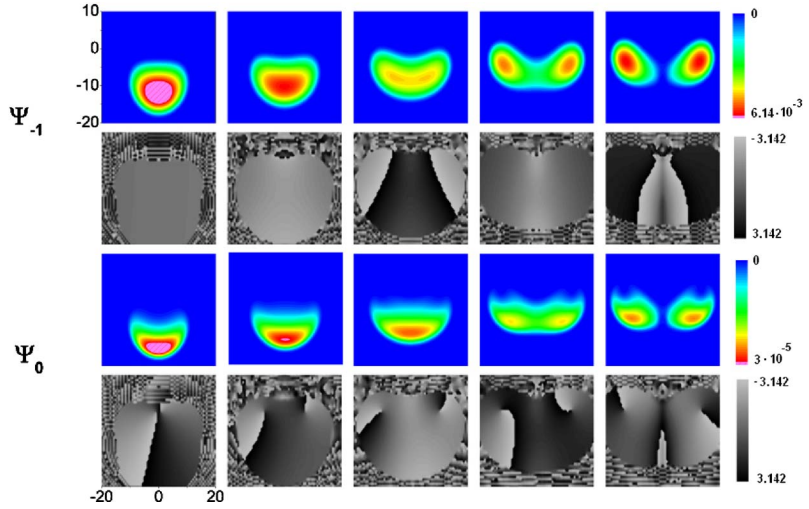

FIG. 2. (Color online) Slow splitting of the condensate by ramping ΔB_x from 0 to 100 mG. Time of splitting about 30 ms. For each component, density and phase profiles are depicted. In the component Ψ_0, singly quantized vortices of topological nature are seen. Their phase singularities reside in the minima of the magnetic field which slowly move as ΔB_x is increased.

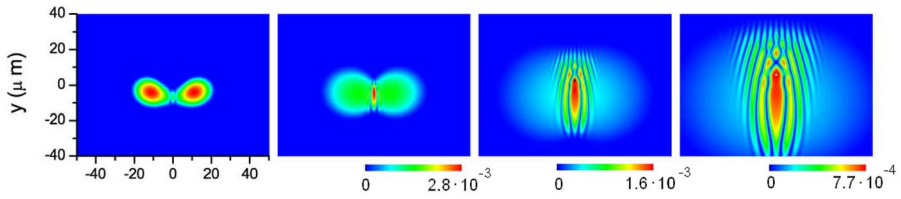

FIG. 3. (Color online) Formation of fringes during expansion of the slowly split condensates. Switching-off of magnetic fields was done in such a way that almost all population (more than 99%) remains in Ψ_{-1} component.

$$F_z = \frac{1}{\sqrt{2}}\begin{pmatrix} 1 & 0 & 0 \\ 0 & 0 & 0 \\ 0 & 0 & -1 \end{pmatrix},$$

and $g_n = 4\pi\hbar^2(a_0+2a_2)/3m$ the spin-independent and $g_s = 4\pi\hbar^2(a_2-a_0)/3m$ the spin-dependent interaction coefficients. Here the scattering lengths a_0 and a_2 characterize collisions between atoms with total spin 0 and 2, m is the atomic mass.

We consider a condensate of ^{23}Na, which was used in the experiment of [2]. Parameters of Na are $M=3.81\times10^{-26}$ kg, $a_2=2.75$ nm, $a_0=2.46$ nm [6]. Spin-independent potential $V(\mathbf{r})$ is determined by gravity: $V(\mathbf{r})=-Mgy$. We assume the wave function of either component is independent of the z coordinate; i.e., the condensate is quasi-2D. We therefore use two-dimensional nonlinearity parameters g_n^{2D} and g_s^{2D}, which are related as $g_n^{2D}/g_s^{2D}=27.44$. The magnetic field configuration is described in the next subsection.

B. The magnetic trap

We use a two-wire setup suggested in Ref. [3]. It was used in a recent experiment of Shin *et al.* [2], where several important elements were added making the system essentially three-dimensional. We consider a two-dimensional trap here to simplify numerical calculations. The magnetic field produced by the two parallel current-carrying wires is given by

$$B_x^W = \frac{-y}{(x+d)^2+y^2} + \frac{-y}{(d-x)^2+y^2},$$

$$B_y^W = \frac{x+d}{(x+d)^2+y^2} + \frac{-d+x}{(d-x)^2+y^2}, \quad (4)$$

where $2d$ is the distance between the wires.

An additional magnetic field B_z is applied along the z direction, and bias field B_x^B is added in the x direction: $B_x=B_x^W+B_x^B$. For weak-field-seeking atoms, the amplitude of magnetic field $B(x,y)$ plays the role of a trapping potential [while the potential for strong field-seeking atoms is $-B(x,y)$]. At certain critical $B_x^B=B_{x_0}$, the trap potential $B(x,y)$ has a single minimum located at a distance d away from the surface, at the middle of the two wires. Depending on the sign of $\Delta B_x \equiv B_x^B - B_{x_0}$ the potential may have two wells: when $\Delta B_x>0$, the two wells are separated in the x direction, while for $\Delta B_x<0$ they are separated in the y direction and their centers have equal x coordinates. Addition of bias magnetic field B_y^B along the y axis rotates these two wells in the xy plane. It is important that the critical single well potential is approximately harmonic (corresponding to a hexapole configuration of the magnetic field), while either of the separated double wells is approximately quadrupole. We assume a uniform B_z is applied to the system. In numerical calculations, we used the parameters close to the experiment of Ref. [2]: $d=150$ μm (this corresponds to the distance between the wires of 300 μm), $B_{x_0}=24$ G, $B_z(0)=1$ G.

C. Strong- and weak-field seeking states in a two-wire trap

The important feature of static magnetic traps is that it confine the weak-field seeking state(s) (WFSS), which has a higher energy than the strong-field seeking state(s) (SFSS). Therefore, there is some difficulty in numerical preparation

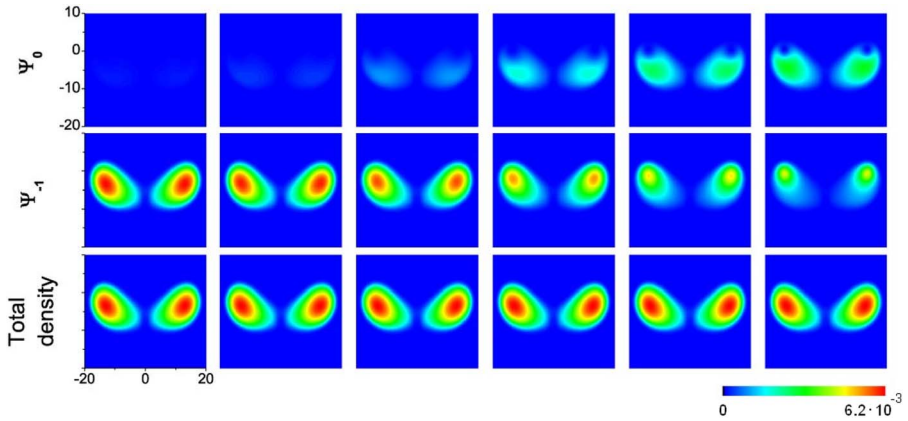

FIG. 4. (Color online) Formation of singly quantized vortices in the Ψ_0 component during switching-off process. B_z decays faster than $B_\perp$. Time of switching-off process is about 20 μs.

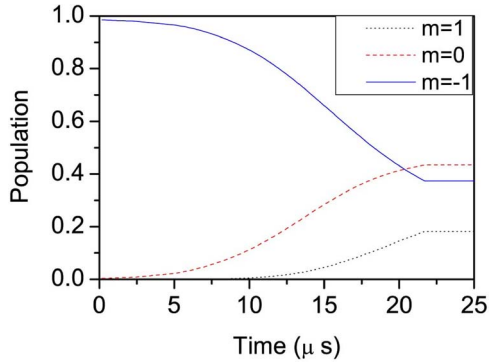

FIG. 5. (Color online) Time evolution of populations of the components of the condensate during switching off. Time of switching-off process T_{off} is about 20 μs (at this time, all the remaining magnetic fields are abruptly turned off).

of initial states, since straightforward imaginary time propagation would lead to SFSS. One need to search for a solution using a WFSS ansatz which is derived from the eigenvector of the $\mathcal{B}$ matrix. The eigenvalues of $\mathcal{B}$ are $\pm B$ (where $B=\sqrt{B_x^2+B_y^2+B_z^2}$) and 0 (the last corresponding to the neutral field-seeking state, NFSS), and the eigenvector corresponding to WFSS is

$$|-1\rangle = \frac{1}{2B}\begin{pmatrix} (B-B_z)(B_x-iB_y)/B_\perp \\ -\sqrt{2}B_\perp \\ (B+B_z)(B_x+iB_y)/B_\perp \end{pmatrix}. \quad (5)$$

Suppose we have a configuration with $\Delta B_x=0$ (so that the wells are coalesced in a single harmonic well). When $(B_x \pm iB_y)/B_\perp = e^{\mp 2i\phi}$ in the vicinity of the minimum of the well, where ϕ is the polar angle around the point of the minimum. The order parameter of the weak-field-seeking state in the vicinity of the minimum of the well has the form

$$\begin{pmatrix} \Psi_1 \\ \Psi_0 \\ \Psi_{-1} \end{pmatrix} = \frac{1}{2B}\begin{pmatrix} (B-B_z)(B_x-iB_y)/B_\perp \\ -\sqrt{2}B_\perp \\ (B+B_z)(B_x+iB_y)/B_\perp \end{pmatrix}\psi e^{iw\phi}$$
$$= \frac{1}{2B}\begin{pmatrix} (B-B_z)e^{2i\phi} \\ -\sqrt{2}B_\perp \\ (B+B_z)e^{-2i\phi} \end{pmatrix}\psi e^{iw\phi}, \quad (6)$$

where ψ is the amplitude (common to all three components). At large B_z, almost all the population is in Ψ_{-1} component. In order to avoid vorticity in this component, we should choose $w=2$. Substituting ansatz (6) into the GP equation, one obtains the one-component equation for the amplitude ψ, which can be solved using imaginary time propagation to find a ground state. However, it is also possible to propagate the original three-component GP equation in the imaginary time, restricting the solution to the anzatz (6). We used both algorithms in our calculations.

One can see that a vortex with vorticity 4 can be obtained from the initial nonvortex state in the critical hexapole trap by a slow reversal of B_z. When $\Delta B_x \neq 0$, we have two quadrupole traps. In that case a slow reversal of B_z leads to doubly quantized vortices in either trap, as was studied in several works recently (for example, Ref. [4]). It is important that the component Ψ_0 in that case contains singly quantized vortices.

III. VORTEX CREATION DURING REALISTIC MAGNETIC TRAP MANIPULATIONS

A. Phase imprinting

In the experiment, the bias fields B_z and B_x^B and the two-wire magnetic field B^W are created by different means. During a switching-off process, they can behave differently. Examples of nontrivial consequences of nonsynchronous decreasing processes of magnetic fields in other situations were considered in Refs. [7,8]. In order to achieve topological imprinting, we consider here the switching-off process

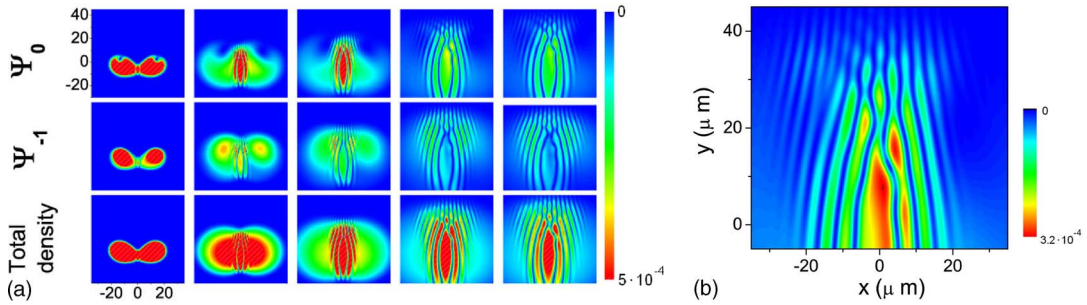

FIG. 6. (Color online) Formation of fringes during expansion of the condensate with imprinted vortices. Almost half of the population were transferred to the component Ψ_0 during switching off. Topological vortices in component Ψ_0 has equal charges in both wells. Only one fork points upward in the Ψ_0 component. In total density pattern, the fork has not appeared yet. However, note that the free expansion took much longer time in the experiment. We see that the Ψ_0 component with vortices rotates clockwise during the expansion. After a long time, the fork therefore might appear in the total density pattern too (our current computational resources forbid such a long-time propagation). (a) Density of components Ψ_0, Ψ_{-1}, and total density. (b) Density of the component Ψ_0 with the fork-like structure after approximately 4 ms of expansion.

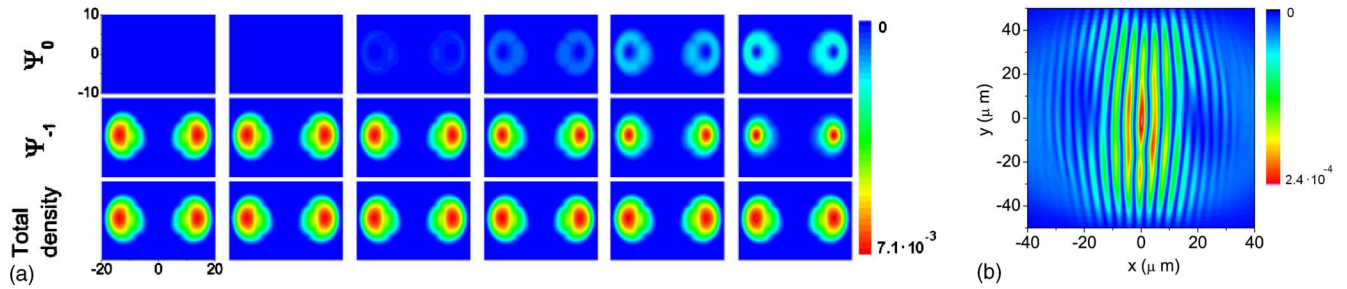

FIG. 7. (Color online) Dynamics without gravity. (a) Formation of singly quantized vortices in Ψ_0 component during switching-off process. B_z decay faster than $B_\perp$. Time of switching-off process was about 20 μs. (b) Fork-like structures in the density of Ψ_0 component.

with B_z decaying faster than $B_\perp$ (in our model calculations, we assume the fields B_x^B and $B_\perp^W$ decay synchronously, while the field B_z decays faster). We found a time of the order of tens of microseconds is enough to transfer a large part of the atoms to component Ψ_0 with singly quantized vortices in each well.

In contrast, we found that in order for the B_z reversal to produce a considerable population of Ψ_1 component with doubly quantized vortices, much longer times are required, i.e., hundreds of microseconds. In the experiment of Ref. [2] switching-off time was $T_{off} \approx 20$ μs. The Larmor frequency at $B=1$ G is ≈ 700 kHz corresponding to $\tau_L \approx 1.4$ μs. Therefore, despite very short switching-off time, "adiabatic" phase imprinting still might take place. We checked this guess numerically.

Four stages of the process were carefully examined: (1) preparation of initial state, (2) splitting, (3) switching-off process, and (4) the free expansion. Firstly, we prepare the initial state in the single (critical) harmonic well using imaginary time propagation, as described in the previous section. (In the real experiment, the condensate was prepared initially at $\Delta B_x = -140$ mG in the bottom well of the double-well potential, but it is not important for our present purpose.) When the condensate was split by ramping ΔB_x from 0 to 100 mG in real time. During this stage, almost all the population is in Ψ_{-1} component, because the B_z field of 1 G is large as compared with magnetic field $B_\perp$ in the vicinity of the minima of magnetic field, where the condensate resides. Provided the splitting is slow, the Ψ_{-1} component remains without vortices (however, at fast splitting it acquires some phase winding, this case is considered in the next subsection). During the third stage, the magnetic field was turned off. Faster decay of B_z may lead to the creation of two *singly quantized* vortices in component Ψ_0 in either of the two wells. This would result in two fork-like structures in the interference pattern of this component [only one of the forks points upward, because charges of the topological vortices in either well are the same (positive)]. The interference fringes were formed during the forth stage of the numerical calculations: the free expansion of the two condensates without magnetic field. For numerical purposes, we also turned off the gravity field in the forth stage, but we suppose this does not influence results significantly. In the real experiment, typical time of expansion was about 22 ms. In our calculations, we typically calculate up to 4 ms only.

In Fig. 1, a fast splitting of the condensate is shown. The condensate was prepared in the merged well (at $\Delta B_x = 0$). The splitting was done approximately in 5 ms, much faster than in the experiment. In Fig. 2, slow splitting of the condensate is monitored (time of splitting is about 30 ms). The final state is slightly different: about 2% of the initial population was lost during the very slow splitting. The atoms that make transitions from WFSS to SFSS fly away (they fly up towards the wires and are removed by absorbing potential on the boundaries of the mesh). The atoms that make transitions to NFSS, fly down because of the gravity (and are also removed).

Densities and phases of the components of the split condensate are presented. Component Ψ_{-1} has no vorticity,

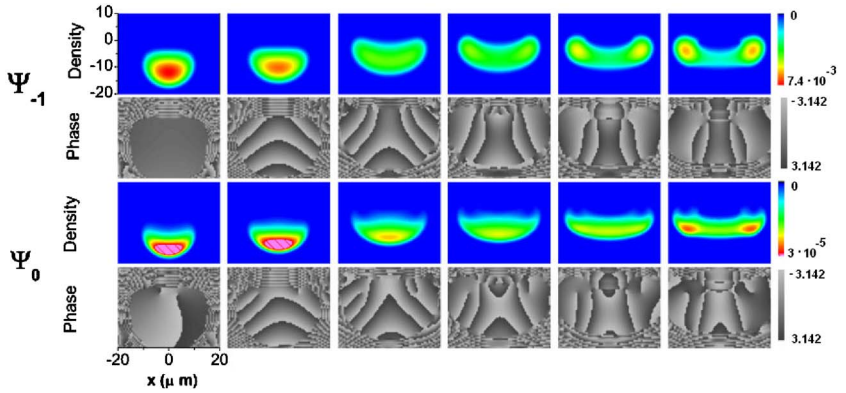

FIG. 8. (Color online) Fast splitting of the condensate. Dynamical formation of vortices: vortices are formed in all components (note that more than 99% of total population is in Ψ_{-1} component). In the Ψ_0 component, dynamical and topological vortices coexist. Topological vortices are the same as in Fig. 2.

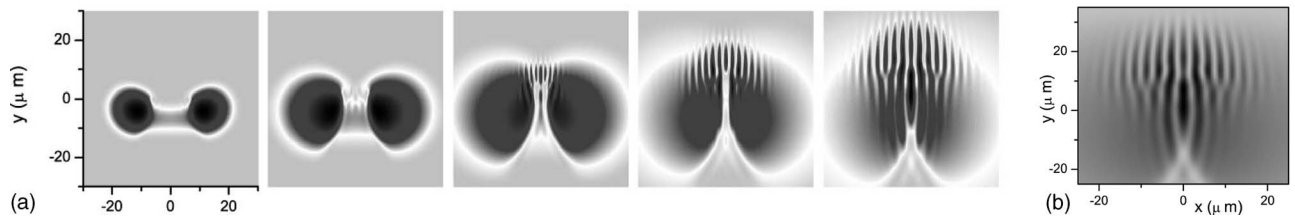

FIG. 9. Formation of fringes during expansion of the rapidly split condensates. During switching off, almost no transfer occur to the component Ψ_0. Dynamical vortices in the two wells have different charges, therefore the two forks point up.

while Ψ_0 has singly quantized vortices in both wells and Ψ_1 has doubly quantized vortices. Since $B_z=1$ G, almost all the population is in the Ψ_{-1} component without vorticity.

In Fig. 3, the interference fringes formed during the free expansion of the condensates are shown. Magnetic fields were switched off in approximately 20 μs in such a way that no transition from Ψ_{-1} component occurred (B_z was decreased more slowly than $B_\perp$).

We now consider a case where B_z is decreasing faster than $B_\perp$. In Fig. 4, the process of topological vortex formation is shown during a switching-off process. Magnetic fields are decreased exponentially, with B_z decaying faster, and are turned off completely at $t=0.06\tau\approx 20$ μs ($\tau\approx 350$ μs is the characteristic time period used in the program). About half of the total population is transferred to the component Ψ_0. An important feature of the nonadiabatic transitions during the switching-off process can be noticed. The part of the condensate in component Ψ_{-1} residing far from the minima of the magnetic field is more easily converted to other components than the part near the minima. As a result, decreasing B_z slices out a part of the condensate around the minima of the magnetic field and leaves it in the initial Ψ_{-1} component. This is due to the fact that in the region where $B_\perp$ is nonzero, a nonvanishing gap between WFSS and NFSS remains; besides, the stronger the field $B_\perp$, the more slowly the total magnetic field rotates, making it easier for the spin of an atom to follow it. Recently, nonadiabatic transitions due to nonsynchronously decreasing trapping magnetic fields (in other configurations) were quantitatively considered in Ref. [7] by generalizing the Landau-Zener formula for the multilevel case. It can be seen also that during the fast switching-off process, the total density is almost unaffected, therefore the nonlinear interaction coefficient g_n plays no significant role in the process.

Time evolution of the population is shown for each in Fig. 5. In Fig. 6, interference fringes formed during the free expansion of the condensates are shown. A fork-like structure is seen in the component Ψ_0.

Topological vortices in the component Ψ_0 in both wells has equal charges. Therefore, only one fork points up in the interference pattern (see Ref. [11]). The Ψ_0 component rotates clockwise during expansion due to equal charge of the vortices and the broken symmetry caused by the gravitational shift, and the fork is moving up. Because of this, although it has not appeared in the total density profile during the time span effected in our calculations, we believe that after a longer time it will show up (note that almost half of the total population is in the Ψ_0 component). The absence of the fork in the total density profile on early stages of expansion is related to the above-mentioned behavior of the switching-off process that leaves Ψ_{-1} component residing near the minima of magnetic field almost unaffected. After the switching-off this component therefore is concentrated at the same places where the phase singularities of component Ψ_0 are located.

For clarity, we give also an example of vortex formation without gravity (Fig. 7). Here, the pair of forks are clearly seen.

B. Dynamical vortex creation

In Fig. 8, a fast splitting of the condensate is monitored. Dynamically created vortices appear in all the components (in component Ψ_0 dynamical and topological vortices coexist). Centers of dynamically created vortices (the phase singularities) lie outside the condensate, but branch cuts go through the condensate causing a phase winding across it. So this situation is different from the so-called ghost vortices appearing in the studies of rotated condensates (Ref. [9]). Although vortices are almost not visible in the density profile of the condensate, its expansion leads to characteristic fork-like structures in the interference fringes due to the phase winding.

The magnetic field was switched off in such a way that almost no transfer to Ψ_0 occur. Thus, Ψ_0 component does not influence the dynamics. In Fig. 9, interference fringes resulted from the subsequent expansion are shown. Two fork-like structures (which appear in all components) are clearly seen. Vortices in the two condensates have opposite charges; therefore, the forks point upward (splitting of the condensate into two parts in the presence of gravity effectively causes a rotation of each part in opposite directions).

To finish off, let us notice that the calculations reported were done using the sin-DVR method (with a spatial mesh of 200×160 grid points), and the time propagation using the Runge-Kutta method (the method is the generalization of the one used in Ref. [10] to the case of spinor condensates). We try to model the system as close to the experimental one as possible. However, we found that, for example, the g_s factor does not affect the results; i.e., the results are qualitatively the same with $g_s=0$. The most important deviation of the model from the experimental system is its reduced dimensionality. The real system is three-dimensional, with nonuniform magnetic fields, with an additional two pairs of wires creating magnetic fields to compensate partly for the nonuniformity of the base magnetic fields and asymmetry, etc. Such a complication is presently beyond our available resources. However, we believe the study of the idealized model do

allow to discuss different mechanisms of vortex creation in the experiment.

IV. CONCLUSION

The authors of the experimental work [2] supposed the phase imprinting mechanism to be unlikely for explaining the appearance of the fork-like structure and that "the observed phase singularity definitely shows the breakdown of adiabaticity." To the contrary, we found a realistic scenario based on nonsynchronous decreasing processes of the magnetic fields can explain the phase singularity even within the assumption of adiabatic evolution.

However, we found that a fast splitting can also lead to dynamical vortex creation, and that the dynamically created vortices produce interference patterns with the forks of better contrast. In other words, both mechanisms are possible (the adiabatic topological and the nonadiabatic dynamical). Detailed study of these processes is left for future research. In any event, the splitting of a spinor BEC is a rather violent process so that further consideration of atom interferometry with spinor BEC is necessary.

ACKNOWLEDGMENTS

A.P.I. is supported by JSPS. This work was also supported in part by Grants-in-Aid for Scientific Research No. 15540381 and 16-04315 from the Ministry of Education, Culture, Sports, Science and Technology, Japan, and also in part by the 21st Century COE program on "Coherent Optical Science." T.M. was also supported in part by a financial aid from the Matsuo Foundation. We would like to acknowledge useful discussions with Prof. Y.S. Kivshar and Prof. Nakagawa.

[1] Y. Shin, M. Saba, T. A. Pasquini, W. Ketterle, D. E. Pritchard, and A. E. Leanhardt, Phys. Rev. Lett. **92**, 050405 (2004).
[2] Y. Shin, C. Sanner, G. B. Jo, T. A. Pasquini, M. Saba, W. Ketterle, D. E. Pritchard, M. Venjalattore, and M. Prentiss, Phys. Rev. A **72**, 021604(R) (2005).
[3] E. A. Hinds, C. J. Vale, and M. G. Boshier, Phys. Rev. Lett. **86**, 1462 (2001).
[4] T. Isoshima, M. Nakahara, T. Ohmi, and K. Machida, Phys. Rev. A **61**, 063610 (2000).
[5] Y. Kawaguchi, M. Nakahara, and T. Ohmi, Phys. Rev. A **70**, 043605 (2004).
[6] D. M. Stamper-Kurn and W. Ketterle, in *Coherent Atomic Matter Waves*, edited by R. Kaiser, C. Westbrook, and F. David (Springer, Heidelberg, 2001).
[7] P. Zhang, Z. Xu, and L. You, Phys. Rev. A **73**, 013623 (2006).
[8] X. Q. Ma *et al.*, e-print cond-mat/0509776 (2005).
[9] M. Tsubota, K. Kasamatsu, and M. Ueda, Phys. Rev. A **65**, 023603 (2002).
[10] O. I. Tolstikhin, T. Morishita, and S. Watanabe, Phys. Rev. A **72**, 051603(R) (2005).
[11] S. Inouye, S. Gupta, T. Rosenband, A. P. Chikkatur, A. Gorlitz, T. L. Gustavson, A. E. Leanhardt, D. E. Pritchard, and W. Ketterle, Phys. Rev. Lett. **87**, 080402 (2001).